

Supporting Information

Failure Modes of Protection Layers Produced by Atomic Layer Deposition of Amorphous TiO₂ on GaAs Anodes

Pakpoom Buabthong,¹ Zachary P. Ifkovits,² Paul A. Kempler,² Yikai Chen,¹ Paul D. Nunez,² Bruce S. Brunshwig,³ Kimberly M. Papadantonakis,² and Nathan S. Lewis^{2,3} *

¹Division of Engineering and Applied Sciences, California Institute of Technology, Pasadena, CA 91125

²Division of Chemistry and Chemical Engineering, California Institute of Technology, Pasadena, California 91125, USA.

³Beckman Institute and Molecular Materials Research Center, California Institute of Technology, Pasadena, California 91125, USA.

*Corresponding author: nslewis@caltech.edu

Estimate of Time to Etch Through GaAs Wafer

The time to etch through the wafer was estimated using Eq. S1, assuming one pinhole orifice with a fixed diameter and isotropic spherical etching. The background current density ($J_{\text{before}} = 0.05 \text{ mA cm}^{-2}$) was subtracted from the steady-state current density after the stepwise increase ($J_{\text{after}} = 0.19 \text{ mA cm}^{-2}$). The electrode area was $A_{el} = 0.068 \text{ cm}^2$. The thickness of the GaAs wafer was $r_{\text{etch}} = 350 \text{ }\mu\text{m}$ ($\rho = 5.32 \text{ g cm}^{-3}$, $N_{\text{GaAs}} = 145 \text{ g mol}^{-1}$, the volume etched was

$$V_{\text{etch}} = \frac{1}{2} \left(\frac{4}{3} \pi r_{\text{etch}}^3 \right)$$

T

(Eq. S1)

$$= \frac{V_{\text{etch}} \rho_{\text{GaAs}} M_{\text{GaAs}} N_{\text{St}} N_A}{(J_{\text{after}} - J_{\text{before}}) A_{el}} \cdot \left(\frac{6 \text{ mol } e^-}{1 \text{ mol}_{\text{GaAs}}} \right) \cdot \left(6.022 \cdot 10^{23} \right) \cdot \left(\frac{1 \text{ cm}^2}{(0.19 - 0.05) \text{ mA}} \right) \cdot \left(\frac{1}{0.068} \right)$$

Dissolution of TiO₂

ICP-MS could not be utilized to monitor analytically the formation of pinholes in the TiO₂ layer by measuring the Ti concentration of the electrolyte. Assuming a pinhole has approximately a 100 nm radius, and the complete formation of a pinhole through the entire layer creates a perfectly cylindrical void, the void would have a volume of $0.1^2 \times \pi \times 0.1 = 0.003 \text{ }\mu\text{m}^3$. This is an *equivalent* volume to $3.14 \times 10^{-15} \text{ cm}^3$. TiO₂ has a density of 4.23 g cm^{-3} , resulting in this representative pinhole having lost a total mass of TiO₂ of $1.3 \times 10^{-14} \text{ g} = 1.3 \times 10^{-5} \text{ ng}$. Titanium represents 60% of the mass of TiO₂, so the mass of titanium from one pinhole is approximately $8 \times 10^{-6} \text{ ng}$. In a solution of 20 mL, this is a concentration of $4 \times 10^{-4} \text{ ng L}^{-1}$, well

below the minimum detection limit of $\sim 1 \text{ ng L}^{-1}$. Furthermore, the sample is diluted with nitric acid during sample preparation, reducing the concentration by an additional order of magnitude.

Challenges in Time-Series Scanning Electron Microscopy (SEM)

Although a time-series SEM can provide insights on the evolution of a new pinhole, sample preparation and transport can alter the surface chemistry and morphology of samples. Figure S8a shows current density as a function of time of $\text{p}^+\text{-GaAs/a-TiO}_2\text{-2000x}$ under operation with a stepwise increase suggesting a new pinhole formation at 7.5 min. Figure S8b shows the corresponding SEM taken after the increase in current density.

The sample was taken out, rinsed with deionized water, and blow-dried with N_2 gas to prevent further corrosion from electrolyte contact. The SEM shows possible film breakage from the preparation step over the corrosion pit. Subsequently, when the sample was put back to electrochemical operation, a substantial increase in the corrosion current density was observed (from 0.7 mA cm^{-2} to 1.4 mA cm^{-2}). The increase in current density is likely due to an increase in the surface area from the torn a-TiO_2 film and oxidized exposed GaAs which is more soluble in 1.0 M KOH(aq) . To accurately monitor the evolution of the pinhole, an operando SEM capability is needed to avoid changing the surface morphology and chemical state during the electrochemical operation.

Supporting Figures

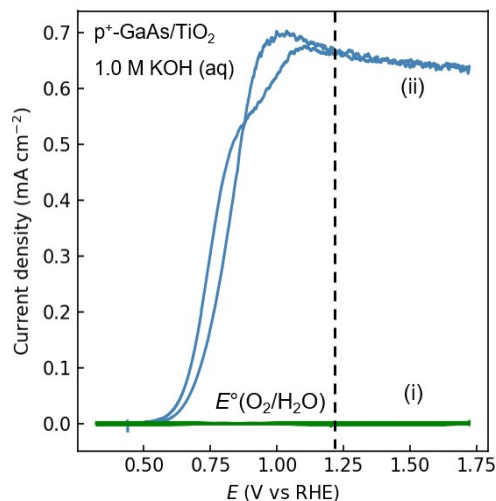


Figure S1. Current density vs potential (J - E) behavior of p^+ -GaAs samples coated with a-TiO₂-2000x (2000 ALD cycles) but without Ni (GaAs/a-TiO₂-2000x). The scan rate was 40 mV s⁻¹. Two types of electrochemical behaviors were observed for the GaAs/a-TiO₂-2000x samples: (i) no apparent corrosion current and (ii) substantial corrosion currents.

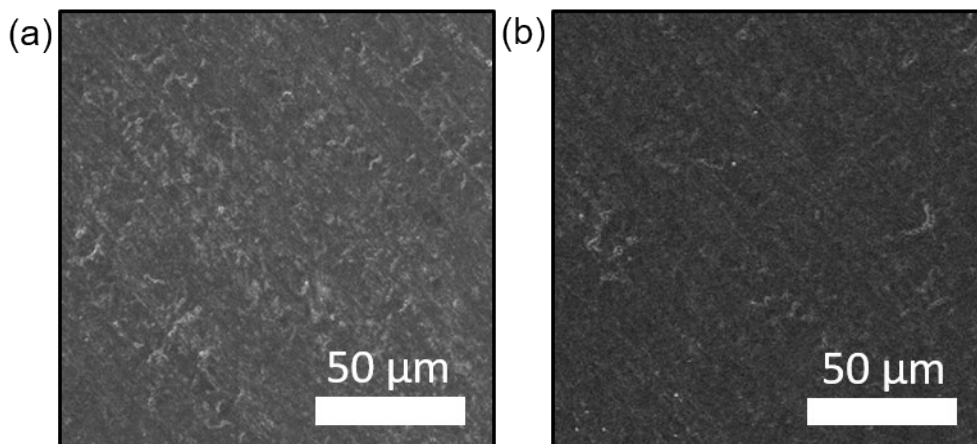


Figure S2. Scanning-electron micrographs of (a) a-TiO₂/Ti foil before Au deposition and (b) a-TiO₂/Ti after Au deposition.

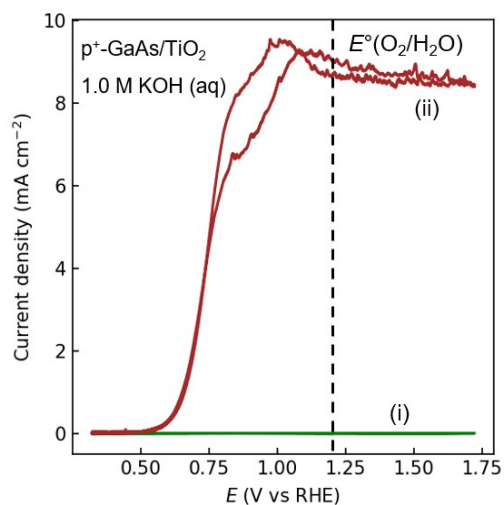


Figure S3. Current density as a function of time for p⁺-GaAs samples coated with a-TiO₂ (2000 ALD cycles) but without Ni (GaAs/ a-TiO₂-2000x) at (i) 0 h and (ii) 1 h. The scan rate was 40 mV s⁻¹.

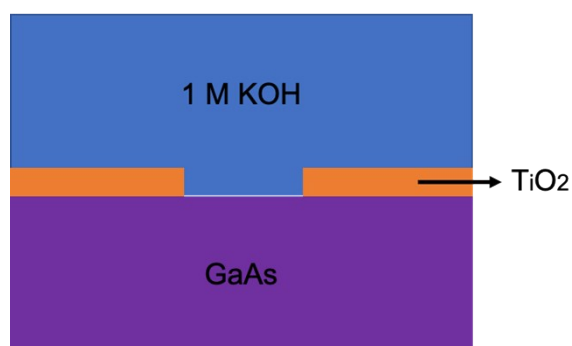


Figure S4. Schematic of the initial geometry used in COMSOL simulation (out of scale).

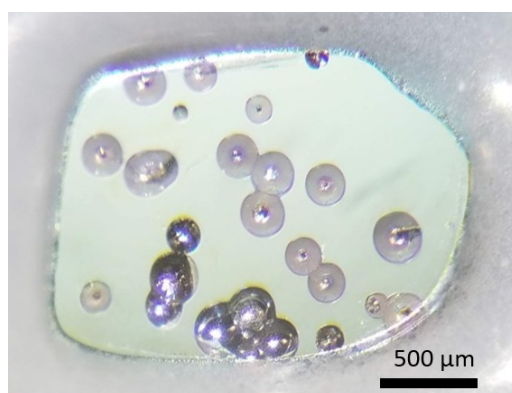


Figure S5. Micrograph of the p⁺-GaAs/TiO₂-2000x after electrochemical testing

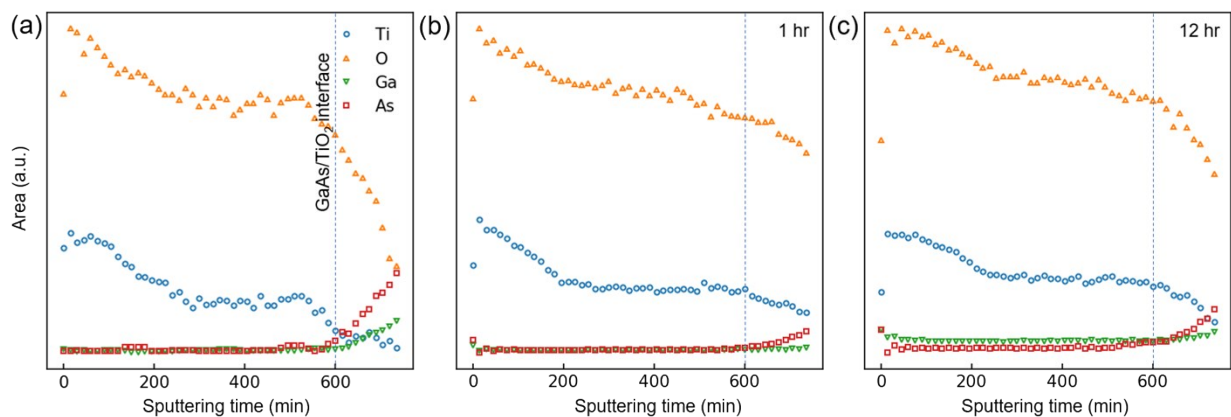


Figure S6. Area of under the peaks for Ti 2p (blue circles), O 1s (orange triangles), Ga 3d (green inverted triangles), and As 3d (red squares) signals as a function of sputtering time on p⁺-GaAs/TiO₂-400x samples measured (a) before testing, (b) 1 h after testing, and (c) 12 h after testing.

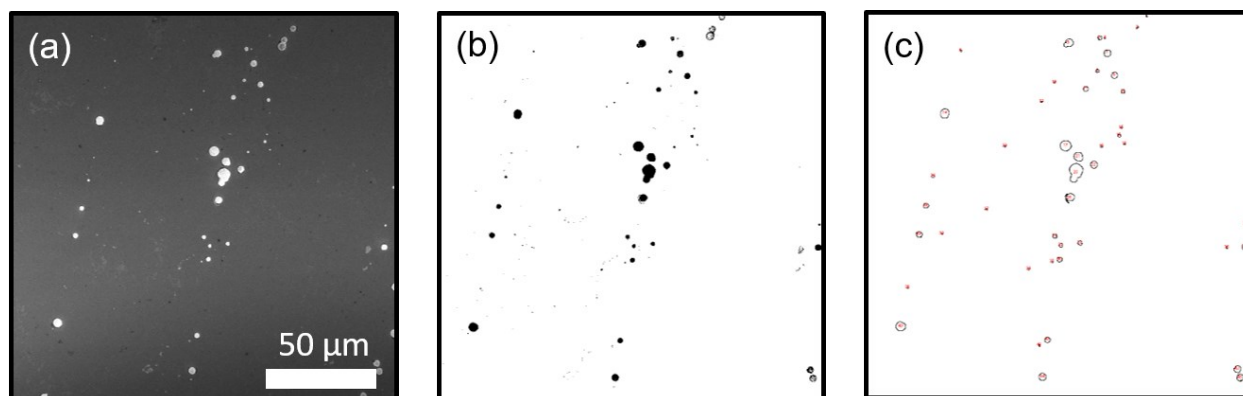


Figure S7. Image processing steps to determine the density of plated Au in pinholes (a) raw scanning-electron micrograph (b) conversion to 8-bit image and (c) outlines of the gold sites counted by the software.

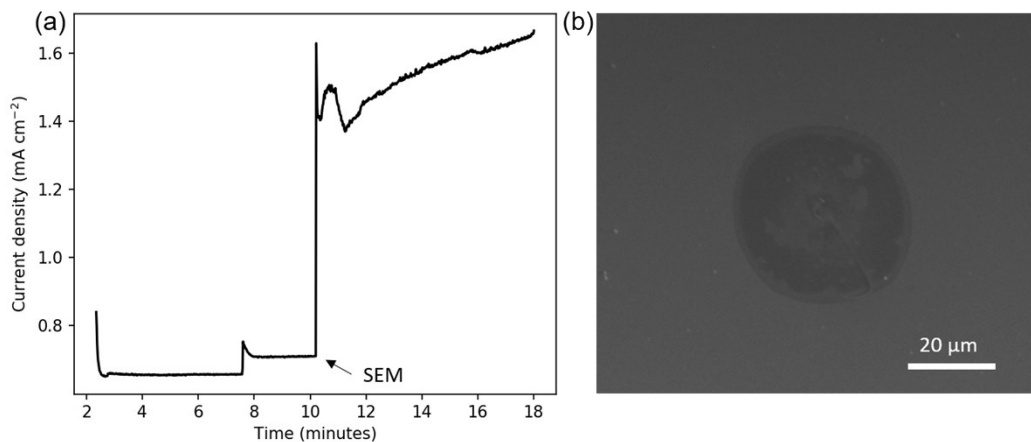


Figure S8. (a) Current density as a function of time of p⁺-GaAs/a-TiO₂-2000x held at 1.13 V vs. RHE in 1.0 M KOH(aq) (b) the corresponding scanning-electron micrograph taken at ~10 min.